ELECTRON TEMPERATURE DETERMINATION FROM THE He I 3889Å AND 5016Å LINE INTENSITIES

Nils Brenning

March 1979

Department of Plasma Physics
Royal Institute of Technology
100 44 Stockholm, Sweden

ELECTRON TEMPERATURE DETERMINATION FROM THE H_eI 3889Å AND 5016Å LINE INTENSITIES

N Brenning

Royal Institute of Technology, Department of Plasma Physics,
S-100 44 Stockholm, Sweden

Abstract

The possibility of determining electron temperature by helium spectroscopy in low-density ($n_e < 10^{20} m^{-3}$) plasmas is discussed. It is concluded that most lines can only be used at very low densities ($n_e < 2 \cdot 10^{16} m^{-3}$) because the line intensities are highly influenced by secondary processes, such as electron impact induced transitions between excited levels or excitations from metastable levels. The density range where measurements are possible can be extended if the influence of these secondary processes on the line intensities can be determined. For most helium I lines this is impossible for lack of atomic data. However, there are two exceptions, the 3889Å ($3^3P \rightarrow 2^3S$) and the 5016Å ($3^1P \rightarrow 2^1S$) lines. The influence from secondary processes on these lines is calculated, and methods are developed which can be used for measurement of electron temperatures $T_e < 100$ eV in plasmas of densities $n_e < 5 \cdot 10^{19} m^{-3}$. The use of the methods is illustrated by a experiment where they have been successfully applied.

1. Introduction

Spectroscopic determination of electron temperature in a plasma is relatively simple when the line intensities are given by either coronal equilibrium or local thermal equilibrium (LTE). Unfortunately, there is a rather large gap in electron density between the regions where these two models can be applied. For He, for example, LTE models cannot be used unless $n_e > 10^{20} m^{-3}$ (de Vries and Mewe, 1966) while coronal excitation balance is achieved only in low-density plasmas of short duration, typical limits being $n_e < 2 \cdot 10^{16} m^{-3}$, $t < 5 \cdot 10^{-6} s$ (Brenning, 1978a). At these low electron densities laser diagnostics does not yet offer an alternative, particularly not for electron temperatures below around 50 eV (1 eV = 11600 K).

When the electron density is too high for coronal excitation balance to apply, the emission of a line is generally the result of an excitation from the ground state followed by a number of collision--induced transitions between excited levels. The influence on the line intensity from these secondary processes can in principle be calculated from the coupled rate equations for population and depopulation of all levels concerned , but usually the result is very uncertain due to uncertainties in the cross sections etc. needed for the calculations. The possible influence of secondary processes is exemplified by the case of helium. Calculations and experiments (Brenning, 1978a,b) show that the line intensities can deviate from what coronal excitation balance would give by as much as a factor of 10. If this can be taken as typical also for other species, it means that the influence from secondary processes on line intensities must be taken into account, if the strengths of the lines are to be used for T_e determination.

Unfortunately, this is generally not possible to do due to lack of necessary atomic data. This can again be exemplified with the case of helium. In spite of the fact that the helium atom is one of the most studied and best known, an accurate calculation of the influence of secondary processes is impossible for most helium lines (Brenning, 1978a).

The present paper examins how two He I lines, that for different reasons are exceptions from this rule, can be used for electron temperature determination in the region between

coronal and local thermal equilibrium. Methods are developed which can be used for measurements of electron temperatures $T_e \lesssim 100$ eV in plasmas of densities $n_e < 5 \cdot 10^{19} m^{-3}$. One possible application is measurements in plasmas that are lightly seeded with helium. Figures 1 and 2 show when each line can be used. Important parameters are the electron temperature and density, the helium density, and the ratio between the experimental time t_{ex} and the time t_r required for build-up of equilibrium metastable population.

For convenient application of the methods the results are summarized in Figures 1-4. Excitation data for the 3889A line is for convenience given in the form of "apparent excitation rate coefficients" S^*_{3889}. This is the excitation rate coefficient with all secondary processes taken into account, so that evaluation of measured line intensities can be made as if line emission were the result of single collisions between electrons and ground-state helium atoms. For the 5016A line, the useful range in Figure 2 is that where secondary processes (in this case, absorption of resonance radiation) can be neglected. Therefore, the ordinary excitation rate coefficient S_{5016} is given for this line (Fig. 4).
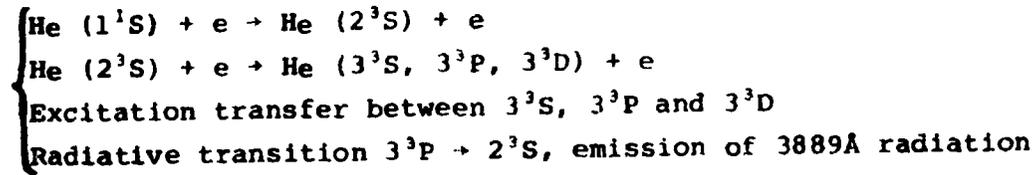
2. The 3889A line

Among the $H_e I$ lines, the 3889A line is unusually well suited for T_e determination due to a combination of circumstances. It is among the very few lines for which the influence of secondary processes can be calculated, since reliable experimental and/or theoretical determinations exist of all the necessary data. Furthermore, it is unusually little influenced by these secondary processes. The fact that it is among the strongest He I lines makes detection possible at low densities.

2.1. Calculations on the 3889A line

The transitions that determine the 3889A line intensity are shown in Figure 5a. The structure becomes a bit clearer of they are separated into the two groups shown in Figures 5b and 5c. The transitions in Figure 5b give the part of the 3889A line emission that is the result of the processes

$\begin{cases} He \ (1^1S) + e \to He \ (3^3S, \ 3^3P, \ 3^3D) + e \\ Excitation \ transfer \ between \ 3^3S, \ 3^3P \ and \ 3^3D \\ Radiative \ transition \ 3^3P \to 2^3S, \ emission \ of \ 3889A \ radiation \end{cases}$

and the transitions in Figure 5c give the line intensity from the processes

$$\begin{cases} \text{He } (1^1S) + e \rightarrow \text{He } (2^3S) + e \\ \text{He } (2^3S) + e \rightarrow \text{He } (3^3S, \ 3^3P, \ 3^3D) + e \\ \text{Excitation transfer between } 3^3S, \ 3^3P \text{ and } 3^3D \\ \text{Radiative transition } 3^3P \rightarrow 2^3S, \text{ emission of } 3889\text{Å radiation} \end{cases}$$

The intensity of the 3889Å line is derived in two steps. First, the population density of the upper line level 3^1P is calculated. this quantity is then used for calculations of the line excitation rate.

2.1.1. 3^1P population due to excitation from the ground state followed by excitation transfer

The populations of the 3^3S, 3^3P and 3^3D levels are in this case given by the coupled rate equations illustrated in Figure 5b:

$$\begin{cases} n_{3^3S} \left(\frac{1}{\tau_{3^3S}} + n_e \, S_{3^3S \rightarrow 3^3P} \right) - n_e n_{3^3P} \, S_{3^3P \rightarrow 3^3S} \, - \\ \quad - \, n_e n_{1^1S} \, S_{1^1S \rightarrow 3^3S} = 0 \hspace{3cm} (1) \\[2mm] n_{3^3P} \left(n_e \, S_{3^3P \rightarrow 3^3S} + n_e \, S_{3^3P \rightarrow 3^3D} + \frac{1}{\tau_{3^3P}} \right) - n_e n_{3^3S} \, S_{3^3S \rightarrow 3^3P} \, - \\ \quad - \, n_e n_{3^3D} \, S_{3^3D \rightarrow 3^3P} - n_e n_{1^1S} \, S_{1^1S \rightarrow 3^3P} = 0 \hspace{1cm} (2) \\[2mm] n_{3^3D} \left(n_e \, S_{3^3D \rightarrow 3^3P} + \frac{1}{\tau_{3^3D}} \right) - n_e \, n_{3^3P} \, S_{3^3P \rightarrow 3^3D} \, - \\ \quad - \, n_e \, n_{1^1S} \, S_{1^1S \rightarrow 3^3D} = 0 \hspace{3cm} (3) \end{cases}$$

This system of equations can be solved to give the part of the 3^3P population that corresponds to excitation from 1^1S followed by excitation transfer:

$$n_{3^3P} \text{ (from } 1^1S) = n_e \, n_{1^1S} \times$$

$$\times \frac{S_{1^1S \rightarrow 3^3P} \left(\dfrac{S_{1^1S \rightarrow 3^3S} \, S_{3^3S \rightarrow 3^3P}}{\dfrac{1}{n_e \tau_{3^3S}} + S_{3^3S \rightarrow 3^3P}} \right) + \left(\dfrac{S_{1^1S \rightarrow 3^3D} \, S_{3^3P \rightarrow 3^3D}}{\dfrac{1}{n_e \tau_{3^3D}} + \left(S_{3^3P \rightarrow 3^3D} \right) \cdot 3/5} \right) \cdot \dfrac{3}{5}}{\dfrac{S_{3^3S \rightarrow 3^3P}}{3} + S_{3^3P \rightarrow 3^3D} + \dfrac{1}{n_e \tau_{3^3P}} - \left(\dfrac{\left(S_{3^3S \rightarrow 3^3P} \right)^2 \cdot \frac{1}{3}}{\dfrac{1}{n_e \tau_{3^3S}} + S_{3^3S \rightarrow 3^3P}} \right) \left(\dfrac{\left(S_{3^3P \rightarrow 3^3D} \right)^2 \frac{3}{5}}{\left(S_{3^3P \rightarrow 3^3D} \right) \frac{3}{5} + \dfrac{1}{n_e \tau_{3^3D}}} \right)} \quad (4)$$

2.1.2 3^1P population due to excitations from the metastable level 2^3S followed by excitation transfer

The population density of the 2^3S level is coupled to the ground state population by the rate equation

$$\frac{d}{dt}(n_{2^3S}) = n_e\, n_{1^1S}\, \Sigma\, S_{1^1S \to 2^3S} - n_e\, n_{2^3S}\, \Sigma\, S_{2^3S \to i,\, 1^1S} \qquad (5)$$

where $\Sigma\, S_{1^1S \to 2^3S}$ denotes the sum of the rate coefficients for all routes of excitation $1^1S \to 2^3S$, and $\Sigma\, S_{2^3S \to i,\, 1^1S}$ denotes the corresponding sum for deexcitation, which gives either an ion or an atom in the 1^1S state. $\Sigma\, S_{1^1S \to 2^3S}$ and $\Sigma\, S_{2^3S \to i,\, 1^1S}$ are given in Figure 5.

We will first treat the case when the 2^3S population is in equilibrium with respect to the ground state population. Equation (5) then gives

$$n_{2^3S}\ \text{(equilibrium)} = n_{1^1S}\ \frac{\Sigma^1\, S_{1^1S \to 2^3S}}{\Sigma^2\, S_{2^3S \to i,\, 1^1S}} \qquad (6)$$

The rate equations for the transitions drawn with solid lines in Figure 5c are very similar to equations (1) to (3) above. They can be combined with (6) and solved to give the part of the 3^3P population that comes from excitation from 2^3S in equilibrium population, followed by excitation transfer:

$$n_{3^3P}\ \text{(from 2^3S in equilibrium)} = n_e\, n_{1^1S}\, \frac{\Sigma\, S_{1^1S \to 2^3S}}{\Sigma\, S_{2^3S \to i,\, 1^1S}} \quad \times$$

$$x\ \frac{S_{2^3S \to 3^3P}\left(\dfrac{S_{2^3S \to 3^3S}\, S_{3^3S \to 3^3P}}{\dfrac{1}{n_e\tau_{3^3S}} + S_{3^3S \to 3^3P}}\right) + \left(\dfrac{S_{2^3S \to 3^3D}\, S_{3^3P \to 3^3D}}{\dfrac{1}{n_e\tau_{3^3D}} + \left(S_{3^3P \to 3^3D}\right)\cdot 3/5}\right)\cdot \dfrac{3}{5}}{\dfrac{S_{3^3S \to 3^3P}}{3} + S_{3^3P \to 3^3D} + \dfrac{1}{n_e\tau_{3^3P}} - \left(\dfrac{\left(S_{3^3S \to 3^3P}\right)^2 \cdot \frac{1}{3}}{\dfrac{1}{n_e 3^3S} + S_{3^3S \to 3^3P}}\right) - \left(\dfrac{\left(S_{3^3P \to 3^3D}\right)^2 \frac{3}{5}}{\left(S_{3^3P \to 3^3D}\right)\frac{3}{5} + \dfrac{1}{n_e\tau_{3^3D}}}\right)} \qquad (7)$$

In some cases the 2^3S population is below the equilibrium value given by equation (6). This can occur either because the metastable atoms diffuse out of the plasma, or because the experimental time is too short for the build-up of equilibrium population. (Reduced relaxation times for build-up of equilibrium po-

pulation of 2^3S have been calculated from equation (5) and are given in table I for reference). In that case it is practical to refer the 3^3P population to that calculated for equilibrium 2^3S population above:

$$n_{3^3P} \text{ (from } 2^3S\text{)} = \frac{n_{2^3S}}{n_{2^3S} \text{ (equilibrium)}} \cdot n_{3^3P} \text{ (from } 2^3S \text{ in equilibrium)} \quad (8)$$

2.1.3 Influence on the 3889Å line intensity from secondary processes

When the line intensity is uninfluenced by secondary processes, the emission rate N_{3889} (photons $m^{-3} s^{-1}$) is determined by the <u>line excitation rate coefficient</u> S_{3889}

$$N_{3889} = n_e \, n_{1^1S} \, S_{3889} \quad (9)$$

The population density of the upper line level is then

$$n_{3^3P} \text{ (no secondary processes)} = n_{1^1S} \, n_e \, S_{1^1S \,\to\, 3^3P} \, \tau_{3^3P} \quad (10)$$

where τ_{3^3P} is the natural lifetime of 3^3P and $S_{1^1S \,\to\, 3^3P}$ is the <u>level</u> excitation rate coefficient, which is connected to S_{3889} by the branching ratio B_{3889} for the line

$$S_{1^1S \,\to\, 3^3P} = B_{3889} \, S_{3889} \quad (11)$$

For the treatment of secondary processes it is convenient to use an expression similar to (9) for the line emission rate:

$$N_{3889} = n_e \, n_{1^1S} \, S^*_{3889} \quad (12)$$

This equation defines the <u>apparent excitation rate coefficient</u> S^*_{3889}.

Since the emission rate of a line is proportional to the population density of the upper line level, the connection between S_{3889} and S^*_{3889} is:

$$S^*_{3889} = S_{3889} \cdot \frac{n_{3^3P}(\text{from } 1^1S) + n_{3^3P}(\text{from } 2^3S)}{n_{3^3P}(\text{no secondary processes})} \quad (13)$$

where the different n_{3^3p}'s are found in equations (4), (7), (8) and (10).

It is now straightforward to calculate S^*_{3889} from the rate co-efficients and lifetimes in these equations. This has been done for electron temperatures 2 eV < T_e < 200 eV (1 eV = 11600 K) and n_e < $10^{20}m^{-3}$. The result is presented in two different ways in Table II and Figures 3a-3f.

Table II gives S^*_{3889}/S_{3889}, which is the factor by which the line intensity is changed compared to the case when secondary processes can be disregarded. This factor typically lies between 0.2 and 4.

The figures give S^*_{3889} for different electron densities and temperatures, and for different population densities for the meta-stable 2^3S level.

2.2 T_e determination from the 3889Å line intensity

A measured line intensity is easiest evaluated in terms of elec-tron temperature with use of the figures 3a-3c. The difference between the figures lies in the 2^3S population. There are two cases for which the evaluation is simple, the first when 2^3S is in equilibrium population with respect to the ground state (Fig. 3a) and the second when excitations from 2^3S can be disregarded (Fig. 3b). Which of the figures that is to be used depends on a comparison between the relaxation time t_r for build-up of equi-librium 2^3S population, the time duration t_{ex} of the experiment and the time t_{diff} it takes a metastable atom to diffuse out of the plasma.

2^3S is in equilibrium population and figure 3a can be used when both $t_{diff} \gtrsim 3 t_r$ and $t_{ex} \gtrsim 3 t_r$. The 2^3S population is so low that excitation from 2^3S can be neglected and figure 3b be used when either $t_{diff} \lesssim 0.1 t_r$ or $t_{ex} \lesssim 0.1 t_r$.

For intermediate 2^3S populations, the problem is more complicated, and one has to integrate the rate equation (5) to determine the 2^3S population density. The graphs in figure 3c can then be used. They give S^*_{3889} for different values of n_{2^3S}/n_{2^3S}(equilibrium). The rate coefficients necessary for the solution of equation (5) are given in Figure 5.

The relaxation time t_r for build-up of 2^3S population is given
in table I for different electron temperatures. The diffusion
time t_{diff} for metastables depends on apparatus size and gas
temperature. If the helium gas is at room temperature and the mean
free path is longer than a characteristic length L, we can appro-
ximate t_{diff} with L/v, where v is the average thermal velocity.
This gives

$$t_{diff} = 7 \cdot 10^{-4} \ L \tag{14}$$

The useful range for the 3889Å line is limited as shown in Figure
1 by two effects. First, the T_e dependence of the rate coefficients
makes the line best suited for T_e determinations below around 20 eV.
Second, the model used here is not correct for too high electron
densities. The reason for this is that for electron densities
approaching $10^{19}m^{-3}$, the 2^3P population density becomes comparable
to the 2^3S population density, and excitations from 2^3P should be
included in the model. Unfortunately, the cross sections for
these transitions are not known well enough for accurate calcu-
lations. The limits to the range of applicability in Figure 1
are based on the uncertainties in these cross sections.

2.3 Choice of data for the calculations

The accuracy of the results obtained above is determined by the
accuracy of the cross sections and lifetimes used to solve equa-
tions (4), (7) and (10). It is therefore necessary to discuss these
in some detail. This is done in Appendix I.

3. The 5016Å line

For the 5016Å line (3^1P-2^1S), the analysis is simpler than for the
3889Å line. The reason for this is that the upper level 3^1P has
a large cross section for excitation from the ground state and a
short natural lifetime. These facts combine to make the intensity
of the 5016Å line very little influenced (always less than 10%)
by secondary processes of the types discussed for the 3889Å line
above. The evaluation of a measured 5016Å line intensity in
electron temperature can therefore be done directly from the line
excitation rate coefficient S_{5016} (Fig. 4).

Unfortunately, the useful range for the 5016Å line is seriously
limited by the fact that the line intensity is dependent on the

degree of imprisonment of resonance radiation. The reason for this
is that the upper line level 3^1P is optically connected to the
ground state. The effect on the line intensity has been calculated
for plane-parallel and cylindrical geometries by Phelps (1958).
Figure 7 shows his results for the intensity of 5016Å radiation
observed perpendicular to a slab of He gas at room temperature
with thickness L. The result can be taken as typical for other geo-
metries, if L is considered as a characteristic length. We find
that the 5016Å line intensity is typically doubled when the pro-
duct $n_{He}L$ is around $2 \cdot 10^{17}$ (m^{-2}). Since it is very complicated
to make corrections for imprisonment, the 5016Å line is easy to
use for T_e determination only when the helium density is below
some critical value, determined by the geometry, electron tempera-
ture, and acceptable uncertainty in the T_e determination. The use-
ful range for the line is therefore limited as shown in Figure 2,
which is obtained by straightforward calculations from the rate
coefficient S_{5016} and Phelp's result for the effect of imprisonment.

Clearly, the 5016 Å line can only be used at substantially lower
helium densities than the 3889 Å line. On the other hand, it can
be used at higher electron densities. The limiting density is
determined by when depopulation of the 3^1P level due to collisions
with electrons is more probable than radiative transfer to the
ground state. The dominating electron collision is in this context
excitation to the n = 4 level. The probability for radiative tran-
sitions to the ground state is influenced by the degree of impri-
sonment of resonance radiation. If $n_{He}L$ is kept below $2 \cdot 10^{17} m^{-2}$
(whithin the "useful range" for the 5016 Å line given in Fig. 2),
the upper limit for the electron density becomes $5 \cdot 10^{19} m^{-3}$.

4. Applications

The use of these diagnostic methods can be illustrated by one
experiment where they have already been applied and one where
application is planned.

4.1 Coaxial plasma gun experiment on the critical ionization ve-
locity. Use of the 3889 Å line

In an experiment by Axnäs (1972, 1978) the critical ionization
velocity is studied. The apparatus is a coaxial plasma gun with
an azimuthal magnetic bias field and a radial discharge current.
The gun is described by Eninger (1966).

The observed phenomenon is that the electric field that can be applied across the discharge is limited to a value which is closely proportional to the magnetic field. This proportionality is maintained over a wide range of experimental parameters. The limiting mechanism is probably connected to some process for enhanced ionization and electron heating. It is essential for the theoretical understanding of the experiment to have measurements of the electron temperature in the discharge. The average electron temperature can be obtained from the ionization relaxation time, which is determined from how the discharge responds to a sudden change in the discharge current (Axnäs, 1972). Langmuir probe measurements are difficult to evaluate, both because of the high magnetic field (0.1 - 1 T), and because the plasma is in the form of a layer that moves axially along the gun with the $\underline{E} \times \underline{B}/B^2$ velocity (typically $10^4 - 5 \cdot 10^4 ms^{-1}$). Another problem is that measurements with probes close to the anode and cathode where sheath formation of some kind could be expected would be uncertain due to the fact that the presence of the probes could disturb such sheaths.

The helium spectroscopic methods were applied to a hydrogen discharge where the average electron temperature (from the ionization relaxation time) is 4 - 5 eV and the electron density around $2 \cdot 10^{18} m^{-3}$ (Axnäs, to be published). This falls within the useful range for the 3889 Å line (Fig. 1).

The relaxation time t_r for build-up of metastable 2^3S population is for the experimental parameters ≈ 9 μs (Table I). This is to be compared to the experimental time t_{ex}, which in this case is the time it takes the current sheath in the discharge to move a distance equal to its own thickness (typically 2 - 3 μs). Since $t_{ex} \approx 0.3\ t_r$, we cannot use the simple evaluation methods (Fig. 3a and Fig. 3b) that are based on either negligible excitation from 2^3S or equilibrium population of 2^3S.

Consequently, the curves in Fig. 3c must be used. Integration of equation (5) shows that the metastable population in a volume of gas gradually builds up from zero to approximately 30% of the equilibrium value $n_{2^3S,\ eq.}$ during the passage of the current sheath. It is not necessary to calculate the precise value as a function of time. Instead the measured line intensities are evaluated for the two limiting cases ($n_{2^3S} = 0$ and $n_{2^3S} = 0.3 \cdot n_{2^3S,\ eq.}$).

This gives a measure of the uncertainty in the temperature deter-
mination due to the unknown 2^3S population.

For the measurements, the neutral gas in the gun was seeded with
a small amount (5%) of helium. This does not alter
the operation of the gun (Axnäs, 1978). The 3889 Å line strength
was measured at different radial positions with a space resolu-
tion of ≈ 2 mm, and the background light (measured with the
same discharge parameters without the addition of helium) was
subtracted.

Evaluation of the measurements revealed an interesting spatial
structure which had escaped detection with other diagnostic
techniques: A thin layer (2 - 3 mm) with a temperature around
5 eV was found near the anode, while the rest of the discharge
(including the region close to the cathode) had an electron
temperature between 2 and 3 eV. The error due to the uncertainty
in the metastable population density was always less than $\pm$ 0.3 eV.

4.2 The electron temperature in a expanding plasma. Use of the 5016 Å line

The dynamics of a plasma injected from an electrodeless plasma gun
into a longitudinal magnetic field has been studied theoretically
by Raadu (1979). An experimental study of the process is being
planned. The apparatus is a conical theta pinch of the type developed
by Bieger et al. (1963), which injects a plasma into a magnetic
field with a field strength of 0.2 T.

From Raadu's theory the temperature is expected to decrease from
around 100 eV to less than 10 eV during the first ten microseconds
of the expansion. At the same time the density decreases from
≈ $2 \cdot 10^{19}$ m^{-3} to ≈ $2 \cdot 10^{18}$ m^{-3}.

The nature of the experiment excludes probe measurements of the
temperature. One problem is the difficulty to make such measure-
ments in a moving plasma (the flow velocity is typically
$4 \cdot 10^5$ m^{-1}), where both the density and the temperature change
rapidly. Another (and perhaps more serious problem) is that
probes would measure the temperature only on magnetic field lines
where the free expansion we want to study is obstracted by the
presence of the probes themselves.

Turning to the spectroscopic methods, we find that the 3889 Å

line is not suited for temperature determination in the predicted parameter range (Fig. 1). Instead the 5016 A line will be used. In order to escape the problem of imprisonment of resonance radiation for temperatures up to 100 eV, the product $n_{He}L$ must be kept below 10^{16} m^{-2} (Fig. 2). Since the drift tube where the plasma expands has a diameter of 5 cm, this condition is fulfilled for $n_{He} = 10^{17}$ m^{-3}. The condition on the electron density $(n_e < 5 \cdot 10^{19})$ is also fulfilled.

In the experiment, the drift tube will be filled uniformly with helium. Calculations on the excitation rate from the rate coefficient (Fig. 4) shows that the line intensity at $n_{He} = 10^{17}$ m^{-3} will be sufficient for time resolution better than 1 µs down to electron temperatures of 10 eV and densities of $2 \cdot 10^{18}$ m^{-3}.

5. Summary

The range of applicability of helium spectroscopy in low density plasma has been extended by three powers of ten in density (from $n_e < 2 \cdot 10^{16} m^{-3}$ to $n_e < 5 \cdot 10^{19} m^{-3}$) by developing methods that quantitatively account for the secondary processes that influence the line intensities. The methods have been summarized in Figs 1-4 in a form appropriate for convenient application. The use of the methods has been illustrated by one experiment where they have already been applied and another where they can be used while other methods can not.

Appendix I Choice of cross sections and lifetimes

Excitations $1^1S \rightarrow 2^3S$

Any excitation to a triplet level leads to an atom in the meta-
stable 2^3S level after cascading. The total $1^1S \rightarrow 2^3S$ cross section
is therefore equal to the sum of all the cross sections for the
triplet levels. This sum is obtained as follows.

For the $1^1S \rightarrow 2^3S$ cross section different experimentalists give
values in good agreement, with a σ_{max} of $3 \cdot 10^{-21} m^2$ between 20
and 30 eV (Scott and Mc Dowell, 1975). For the $1^1S \rightarrow 3^3S$,
$1^1S \rightarrow 4^3S$ and $1^1S \rightarrow 5^3S$ cross sections, values are taken from
St John et al (1963). The relative values of these $1^1S \rightarrow n^3S$ cross
sections agree well with theory (Moustafa Moussa et al, 1969),
which predicts that the excitation cross sections for levels with
the same ℓ quantum number should vary as n^{-3}. This extrapolation,
which is expected to be best for high-lying levels, is used to
obtain cross sections for n^3S levels with $n \geq 6$.

For the n^3P levels, experimentally obtained values are less com-
plete. St John et al (1963) gives a cross section for the 3^3P
level excitation which is used as basis for a n^{-3} extrapolation to
the other n^3P levels. The accuracy of the extrapolation is
probably rather good also for low n quantum numbers in helium. (The
good agreement with measured $1^1S \rightarrow n^3S$ cross sections was mentioned
above. Moust fa and Moussa et al (1969) have also reported close
to n^{-3} variation of the $1^1S \rightarrow n^1P$ (n = 2-5) cross sections.)

The cross sections for 3^1D, 4^1D, 5^1D and 6^1D excitations have
been measured by St John et al (1963). For higher n, the n^{-3}
extrapolation is used.

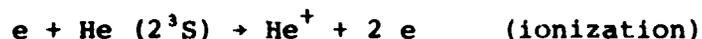In the total $1^1S \rightarrow 2^3S$ cross section obtained by the summation
of the cross sections above, around 33% comes from direct exci-
tation to the 2^3S level. Only around 2% comes from levels with
n > 5. The extrapolations therefore influence the result only marginally.

An experimental determination of the total cross section was done
by Bogdanova and Marusin (1975) with the use of an excitation
exchange mechanism in a He-Cd mixture. The'r value agrees well
with the one obtained here for electron energies below 50 eV.
For higher energies they report values which probably are too
high due to excitation transfer from more easily excited singlet
levels to the triplet system, followed by cascading to 2^3S
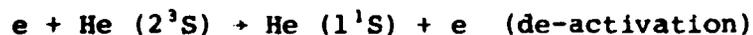
(Brenning, 1978a).

De-excitation from 2^3S

The two dominating de-excitation processes from the 2^3S level are

$$e + He\ (2^3S) \rightarrow He^+ + 2\ e \qquad \text{(ionization)}$$

and

$$e + He\ (2^3S) \rightarrow He\ (1^1S) + e \quad \text{(de-activation)}$$

The former process is studied theoretically by Ton-That et al (1977), who find cross section values in good agreement with the values measured by Dixon et al (1976). The second process is studied by Nesbet et al (1974). It is negligible compared to ionization.

Excitations from 2^3S to 3^3S, 3^3P, 3^3D and 2^3P

The most reliable estimates of these cross sections are probably those by Flannery and Mc Cann (1975) . They use a ten-channel eikonal model for the transitions, which has provided a satisfactory account of integral and differential cross sections for other e-He collision cross sections.

Excitations from 1^1S to 3^3S, 3^3P and 3^3D

Absolute measurements of all three cross sections from threshold to 500 eV have been made by St John et al (1963). Moustafa Moussa et al (1969) have also measured all three cross sections, but only for energies above 80 eV. Showalter and Kay (1975) have measured the $1^1S \rightarrow 3^3P$ and the $1^1S \rightarrow 3^3D$ cross sections for electron energies above 50 eV. These experimentalists report values in agreement for the absolute values for the cross section in the energy range of interest here (below 200 eV). The detailed structure of the cross sections close to threshold is taken from the measurements by Smit et al (1963).

Excitation transfers $3^3S \rightleftarrows 3^3P$ and $3^3P \rightleftarrows 3^3D$

For these transitions, we use the Born-Bethe approximation, as given by Drawin (1966):

$$\sigma_{ij} = 4\pi\ \frac{E_i^H}{E_{ij}}\ |z_{ij}|^2 \left(\frac{E_{ij}}{E_e}\right)^2 \left(\frac{E_e}{E_{ij}} - 1\right) \ln\left(1.5\ \frac{E_e}{E_{ij}}\right) \qquad (14)$$

where E_i^H is 13.59 eV, E_e is the electron energy, E_{ij} is the energy difference $|E_i - E_j|$ between the levels i and j, and z_{ij} is the dipole length for the transition $i \rightleftarrows j$. The dipole lengths

for these transitions in excited helium are very close to the
corresponding dipole lengths for hydrogen, which are used instead.
Values are given by Bethe and Salpeter (1957). The accuracy of
the Born-Bethe approximation is tested against the more sophisti-
cated calculation done for the $2^3S - 2^3P$ transition by Flannery
et al (1975). The two calculations agree within 20%, when the
electron energy is greater than a few times the threshold energy.
The agreement is probably even better for the higher-lying transi-
tions $3^3S \rightleftarrows 3^3P$ and $3^3P \rightleftarrows 3^3D$, where the threshold energies are
much lower and the hydrogen dipole lengths are better approxima-
tions.

Calculations of rate coefficients

Rate coefficients for the transitions were obtained by numerical
integration of close analytical fits to the cross sections above
over Maxwellian electron distributions. The choise of analytical
fits is discussed in Appendix II.

Lifetimes of the 3^3S, 3^3P and 3^3D levels

These are taken from the measurements made by Bukow et al (1977),
which also agree well with theoretical values.

Appendix II Analytical fits to known cross sections

A function which can be adjusted to fit most cross section is:

$$\sigma(w_e) = K_1 \underbrace{\frac{\frac{w_e}{w_T} - 1}{\left(\frac{w_e}{w_T}\right)^2} \, \ln\left(K_2 \, \frac{w_e}{w_T}\right)}_{1} \underbrace{\left(1 + \left(\frac{w_e}{w_{K_1}}\right)^{s_1}\right)^{\frac{\alpha_1}{s_1}}}_{2} \underbrace{\left(1 + \left(\frac{w_e}{w_{K_2}}\right)^{s_2}\right)^{\frac{\alpha_2}{s_2}}}_{3}$$

It is composed of three parts:

Part 1 is the <u>generalized cross section</u> given by Drawin (1966).
W_e is the electron energy, w_T is the threshold energy for the
transition in question, and K determines the absolute value of the
cross section. K_2 influences the shape of the cross section, and
is choosen to give the best fit between threshold and maximum.
K_2 must always be greater than 1.

Parts 2 and 3 are used to adjust the cross section for energies
above maximum. Each gives a "knee" with the following properties.

- For $w_e \ll w_K$, the cross section is multiplied by 1.
- For $w_e \gg w_K$, the cross section is multiplied by $(w_e/w_K)^\alpha$
- s gives the sharpness of the "knee" at $w_e = w_T$.

Parameters for analytical fits of this form used in the calcula-
tions in Section 3 are given in Table III. An example of how the
analytical expressions fit the cross sections is given in Figure 8.

References

Axnäs, I.: 1972, Experimental Investigation of an Ionizing
    Wave in a Coaxial Plasma Gun. Royal Institute of Technology,
    report TRITA-EPP-72-31.

Axnäs, I.: 1978, Experimental Comparison of the Critical Ionization
    Velocity in Atomic and Molecular Gases.

Axnäs, I.: To be published.

Bethe, H.A. and Salpeter, E.E.: 1957, Quantum Mechanics of One
    and Two Electron Systems. Handbuch der Physik 35, p. 349.

Bieger, W., Gresser, H., Noll, P. and Tuczek, H.I.: 1963,
    Z. Naturforschung 18a, 453.

Bogdanova, I.P. and Marusin, V.D.: 1975, Determination of the
    Efficiency of Electron-Impact Excitation of a Metastable 2^3S
    Helium Level. Opt. Spektrosk. 38, 189.

Brenning, N.: 1978a, Electron Temperature Measurements in Low
    Density Plasmas by Helium Spectroscopy II - Parameter Limits
    for Validity of Different Methods. Royal Institute of Techno-
    logy, report TRITA-EPP-78-16.

Brenning, N.: 1978b, Horizontal Thermal Equilibrium due to Exci-
    tation Transfer between Excited States of Neutral He in
    Transient Plasma. J. Phys. B.: Atom. Molec. Phys. 11, L353.

Bukow, H.H., Heine, G. and Reinke, M.: 1977, Lifetime Measurements
    on Atomic States of He I. J. Phys. B.: 10, 2347.

de Vries, R.F. and Mewe, R.: 1966, Spectroscopic Determination of
    Electron Temperature in a Helium Plasma. Phys. Fluids 9, 414.

Dixon, A.J., Harrison, M.F.A. and Smith, A.C.H.: 1976, Ionization
    of He (2^3S) by Electron Impact. J. Phys. B.: Atom. Molec.
    Phys. 9, 2617.

Drawin, H.W.: 1966, Collision and Transport Cross Sections, EUR-
    CEA-FC-383 (Fontenay-aux-Roses).

Eninger. J.: 1966, Experimental Investigation of an Ionizing
    Wave in Crossed Electric and Magnetic Fields. Proc. VII
    Intern. Conf. on Phenomena in Ionized Gases, 1, 520.

Flannery, M.R. and Mc Cann, K.J.: 1975, Ten-channel Eikonal Treatment of Electron-Metastable-Helium Collisions: Differential and Integral Cross Sections for $2^{1,3}P$ and n = 3 Excitations from He $(2^{1,3}S)$ and the (λ, χ, π) parameters. Phys. Rev. $\underline{12}$, 846.

Flannery, M.R., Morrison, W.F., and Richmond, B.L.: 1975, Excitation in Electron-Metastable Helium Collisions. J. Appl. Phys. $\underline{46}$, 1186.

Moustafa Mousa, H.R., de Heer, F.J. and Schutten, J.: 1969, Excitation of Helium by 0.05 - 6 keV Electrons and Polarization of the Resulting Radiation. Physica $\underline{40}$, 517.

Nesbet, R.K., Oberoi, R.S. and Bardsley, J.N.: 1974, Deactivation of He(2^3S) by Thermal Electrons. Chem. Phys. Lett. $\underline{25}$, 587.

Raadu, M.A., 1979, Expansion of a Plasma Injected from an Electrodeless Gun along a Magnetic Field. Plasma Physics $\underline{21}$, 331.

Scott, T. and Mc Dowell, M.R.C.: 1975, Electron Impact Excitation of n^1S and n^3S States of He at Intermediate Energies. J. Phys. B. $\underline{11}$, 1851.

Showalter, J.G. and Kay, R.B.: 1975, Absolute Measurement of Total Electron-Impact Cross Sections to Singlet and Triplet Levels in Helium. Phys. Rev. A, $\underline{11}$, 1899.

Smit , C., Heideman, H.G.M., and Smit, J.A.: 1963, Relative Optical Excitation Functions of Helium (Excitation by Electrons). Physica $\underline{29}$, 245.

St John, R.M., Miller, F.L., and Lin, C.C.: 1964, Absolute Electron Excitation Cross Sections of Helium. Phys. Rev. $\underline{134}$, 888.

Ton-That, D., Manson, S.T. and Elannery, M.R.: 1977, Cross Sections for Excitation and Ionization in e-He $(2^{1,3}S)$ Collisions. J. Phys. B.: $\underline{10}$, 621.

T_e [eV] (1eV=11600K)	2	5	10	20	50	100	200
$n_e \, t_r$ [$m^{-3}s$]	$7 \cdot 10^{13}$	$1.7 \cdot 10^{13}$	$7.7 \cdot 10^{12}$	$6.3 \cdot 10^{12}$	$5.7 \cdot 10^{12}$	$6.3 \cdot 10^{12}$	$6.7 \cdot 10^{12}$

Table I: Reduced relaxation times $n_e \, t_r$ [$m^{-3}s$] for build-up of equilibrium population of 2^3S. (Sections 2.1.2 and 2.2.)

T_e [eV] \ n_e [m^{-3}]	10^{14}	10^{16}	10^{17}	$5 \cdot 10^{17}$	10^{18}	$2 \cdot 10^{18}$	$5 \cdot 10^{18}$	10^{19}	$2 \cdot 10^{19}$	10^{20}
2	3.89	3.89	3.90	3.81	3.65	3.38	3.01	2.78	(2.62)	(2.48)
5	2.84	2.84	2.87	2.96	2.77	2.60	2.33	2.16	(2.04)	(1.93)
10	2.19	2.19	2.17	2.10	2.00	1.84	1.62	1.48	(1.38)	(1.29)
20	2.16	2.15	2.10	1.93	1.79	1.61	(1.34)	(1.22)	(1.11)	(1.01)
50	2.44	2.43	2.35	2.09	1.90	1.67	(1.37)	(1.17)	(1.04)	(0.90)
100	2.54	2.53	2.45	2.20	1.99	1.74	(1.38)	(1.16)	(0.98)	(0.80)
200	2.75	2.74	2.66	2.38	2.16	1.87	(1.46)	(1.19)	(0.98)	(0.75)

Table IIa

T_e [eV] \ n_e [m^{-3}]	10^{14}	10^{16}	10^{17}	$5 \cdot 10^{17}$	10^{18}	$2 \cdot 10^{18}$	$5 \cdot 10^{18}$	10^{19}	$2 \cdot 10^{19}$	10^{20}
2	1.00	0.99	0.89	0.67	0.55	0.43	0.32	0.26	0.22	0.19
5	1.00	0.99	0.91	0.72	0.60	0.48	0.35	0.28	0.24	0.20
10	1.00	0.99	0.92	0.74	0.62	0.49	0.35	0.28	0.23	0.19
20	1.00	0.99	0.93	0.76	0.64	0.51	0.37	0.29	0.23	0.18
50	1.00	0.99	0.94	0.78	0.67	0.54	0.39	0.30	0.23	0.17
100	1.00	1.00	0.95	0.82	0.71	0.59	0.43	0.32	0.25	0.17
200	1.00	1.00	0.96	0.83	0.73	0.60	0.43	0.32	0.24	0.16

Table IIb

Table II: S^*_{3889}/S_{3889} (the factor by which the line intensity is changed by secondary processes) for two cases.

Table IIa: equilibrium population of $2\,^3S$.

Table IIb: zero population of $2\,^3S$. The values are put in parenthesis when they should not be used for T_e determination due to unknown influence from excitations from $2\,^3P$. (Section 2.1.3)

Transition	K_1	K_2	W_T	W_{K_1}	α_1	s_1	W_{K_2}	α_2	s_2
$2^3S \to 3^3S$	$1.77 \cdot 10^{-20}$	100	2.7	70	-0.15	2	0	0	0
$2^3S \to 3^3P$	$6.5 \cdot 10^{-21}$	100	2.7	15	0.8	4	70	-0.7	4
$2^3S \to 3^3D$	$3.3 \cdot 10^{-19}$	1	2.7	10	-0.45	2	0	0	0
$2^3S \to$ ionization	$2.4 \cdot 10^{-21}$	1.5	4.7	0	0	0	0	0	0
$2^3S \to 2^1P$	$2.5 \cdot 10^{-20}$	1	1.14	0	0	0	0	0	0
$3^3S \to 3^3P$	$8.9 \cdot 10^{-17}$	1.5	0.29	0	0	0	0	0	0
$3^3P \to 3^3P$	$1.8 \cdot 10^{-16}$	1.5	0.06	0	0	0	0	0	0

Table III: Parameters for analytical fits to cross sections used
in Section 2.
(Appendix II)
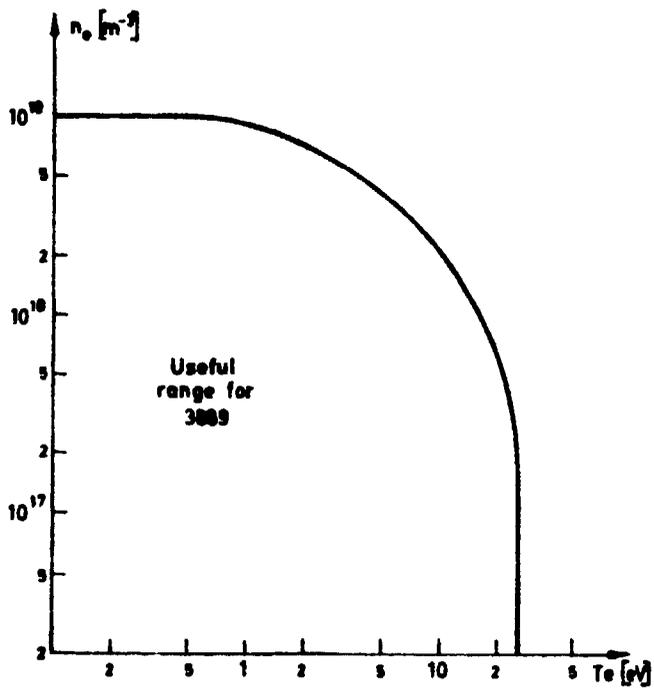
Fig. 1
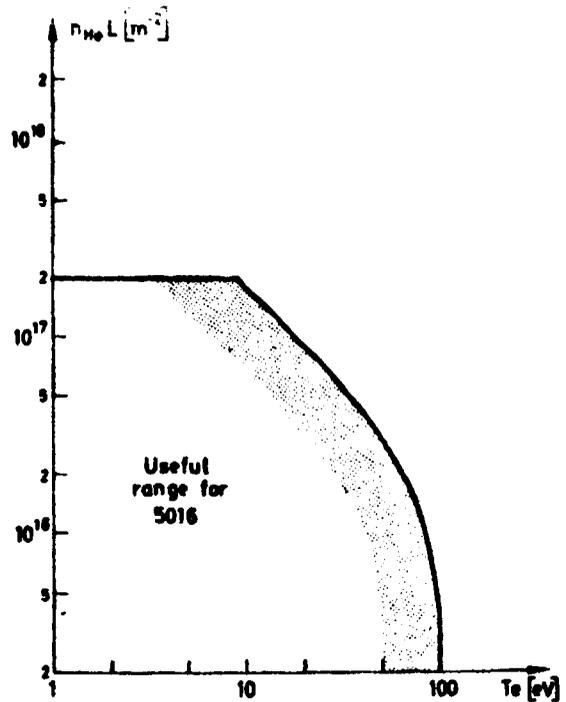
Fig. 2

Figure 1. The usefulness of the 3889Å line is limited by
   approximate upper limits on n_e and T_e as shown in the
   figure. The use of the line depends on the population
   density of the metastable level 2^3S, which can be esti-
   mated from a comparison between the time duration t_{ex} of
   an experiment, the time t_{diff} it takes a metastable atom to
   diffuse out of the plasma and the relaxation time t_r for build-
   -up of equilibrium 2^3S population density (Table I). There are
   three cases:

1) $t_{ex} \gtrsim 3\ t_r$ and $t_{diff} \gtrsim 3\ t_r$. 2^3S is in equilibrium popula-
tion with respect to the ground state. Figure 3a is used for T_e
determination.

2) $t_{ex} \lesssim 0.1\ t_r$ or $t_{diff} \lesssim 0.1\ t_r$. The 2^3S population is negli-
gible. Figure 3b is used for T_e determination.

3) t_{ex} is between the values above. T_e determination is
more complicated, and the reader is referred to Section
2 of the text.

Figure 2. The usefulness of the 5016Å line is limited by
   approximate upper limits on T_e and on the product $n_{He}L$
   (L = typical length) as shown in the figure. For parame-
   ters in the "useful range" T_e is obtained from measured
   line intensities with the use of the excitation rate co-
   efficient S_{5016} in Figure 4. For parameters in the shaded
   area, this gives an overestimate of T_e with 10-30% (Sec-
   tion 3). The electron density must be below $5 \cdot 10^{19}\ m^{-3}$.
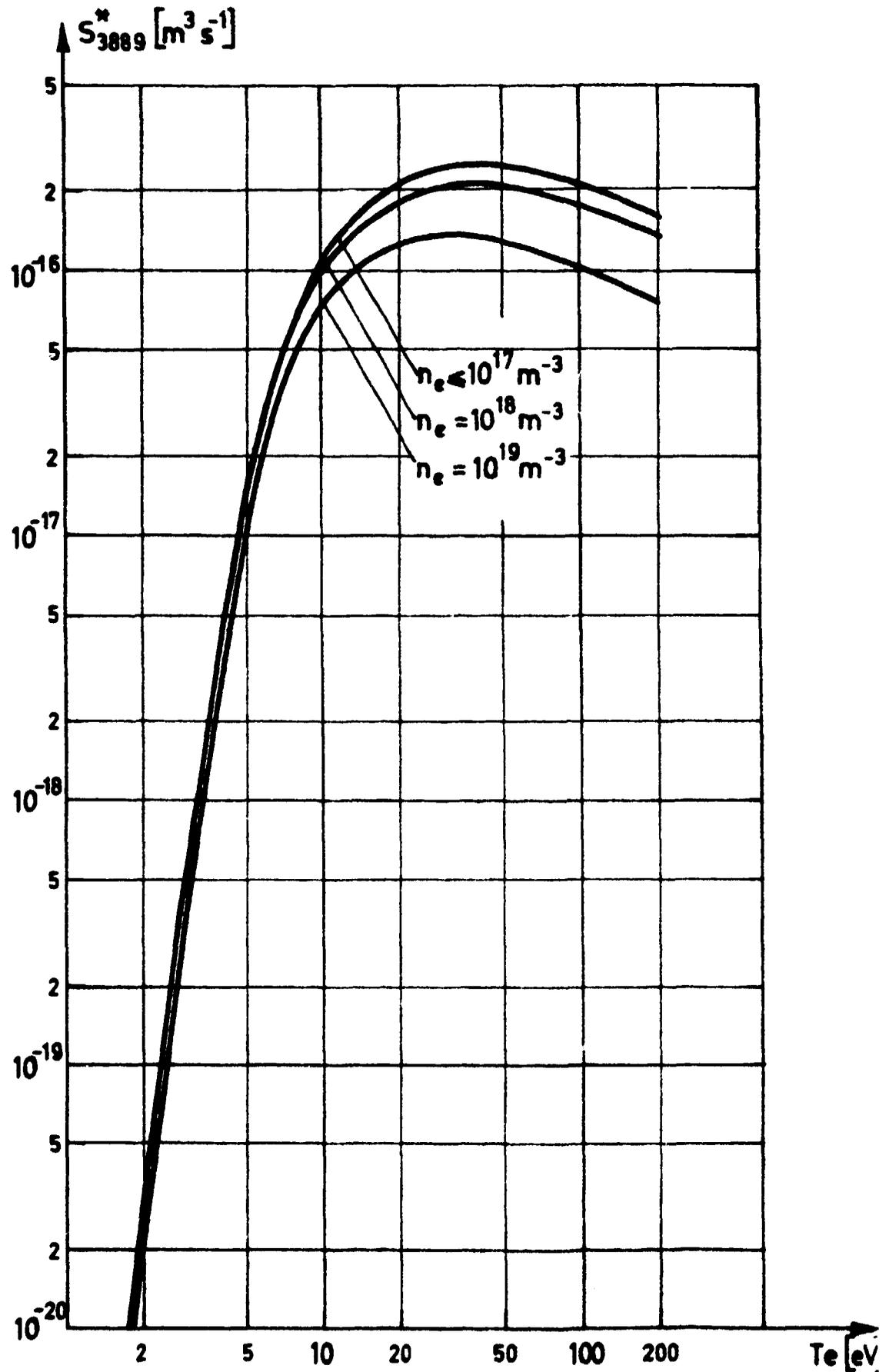
Figure 3a. Apparent excitation rate coefficient (photons $m^{-3}s^{-1}$) for the 3889Å line when 2^1S is in equilibrium population with respect to the ground state.
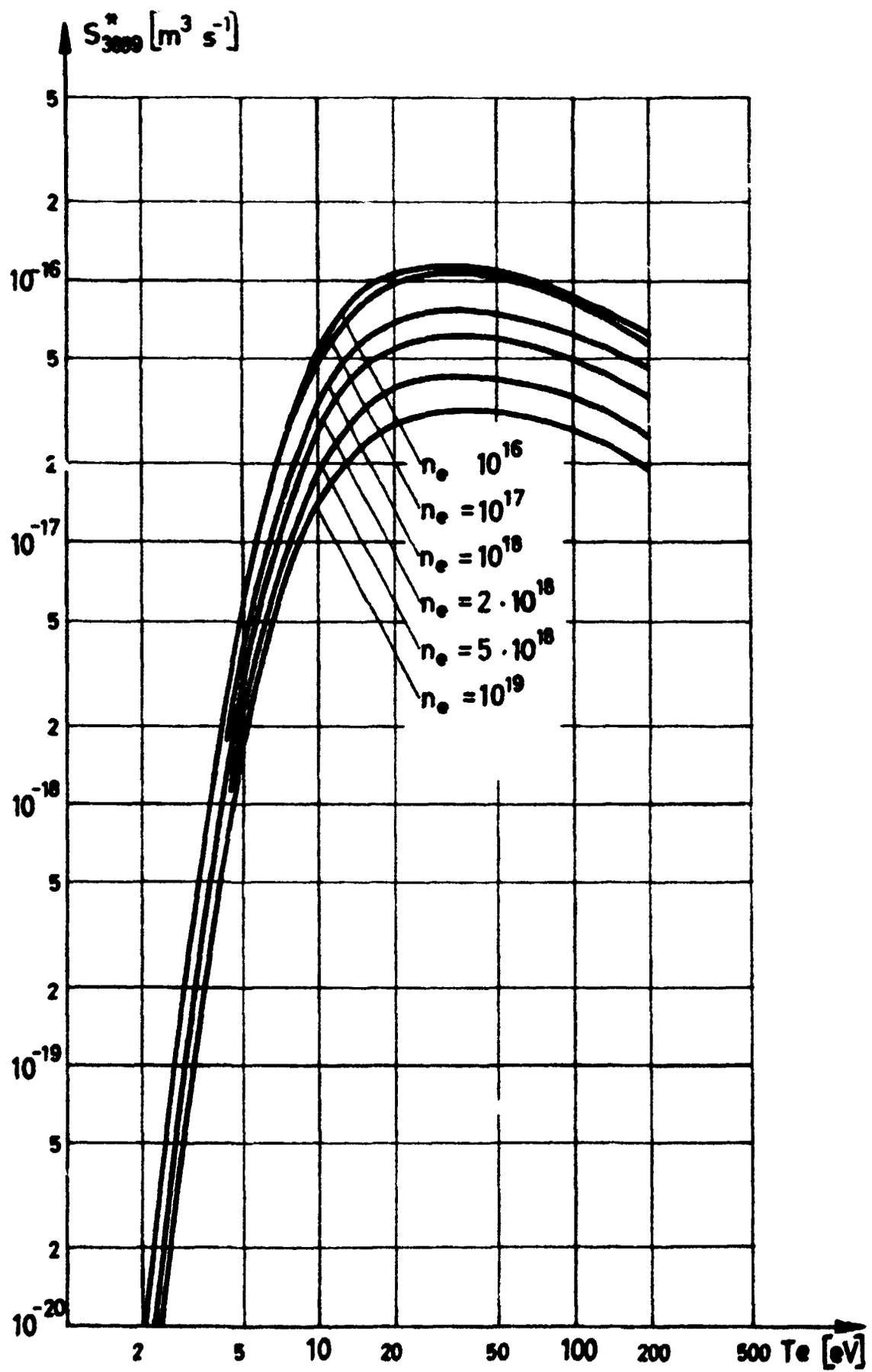
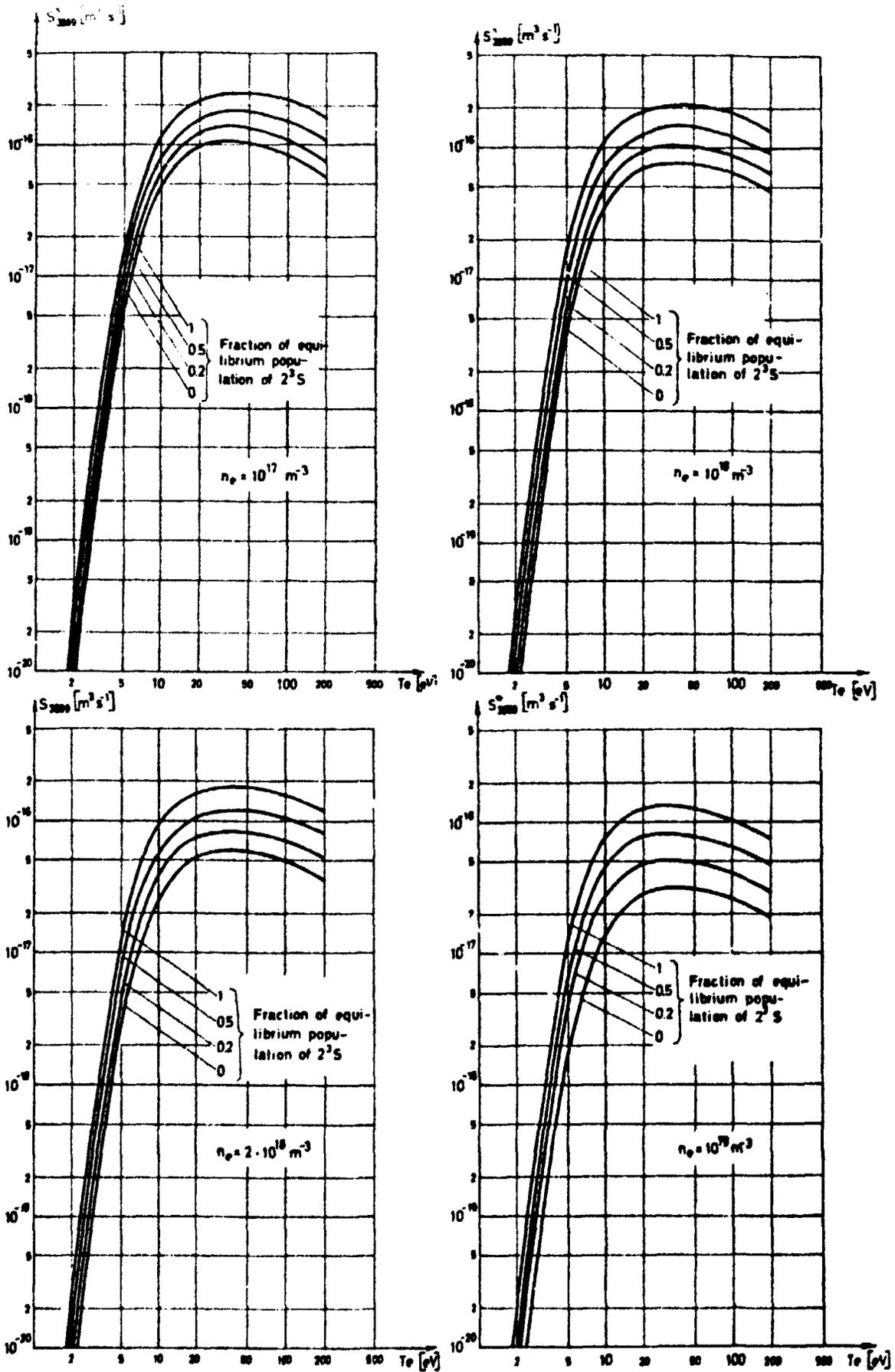Figure 3b. Apparent excitation rate coefficient (photons $m^{-3}s^{-1}$) for the 3889Å line when excitations from $2^{1}S$ can be neglected.

Figure 3c . Apparent excitation rate coefficients (photons m^{-3}s^{-1}) for the 3889 Å line for different fractions of equilibrium population of 2^{3}S. The different figures correspond to different values of n$_e$.
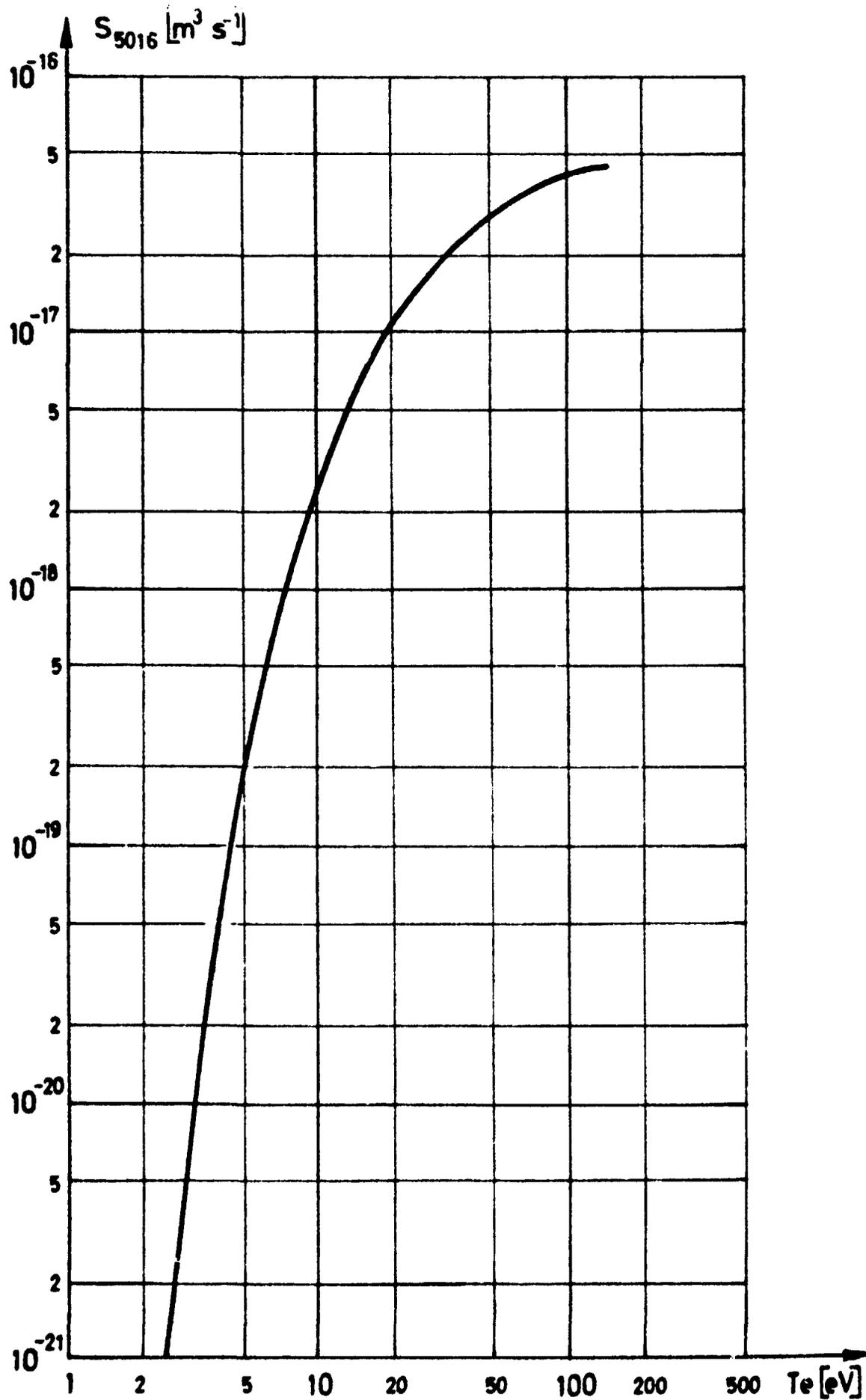
Figure 4. Excitation rate coefficient (photons $m^{-3}s^{-1}$) for the 5016Å line as a function of the electron temperature.
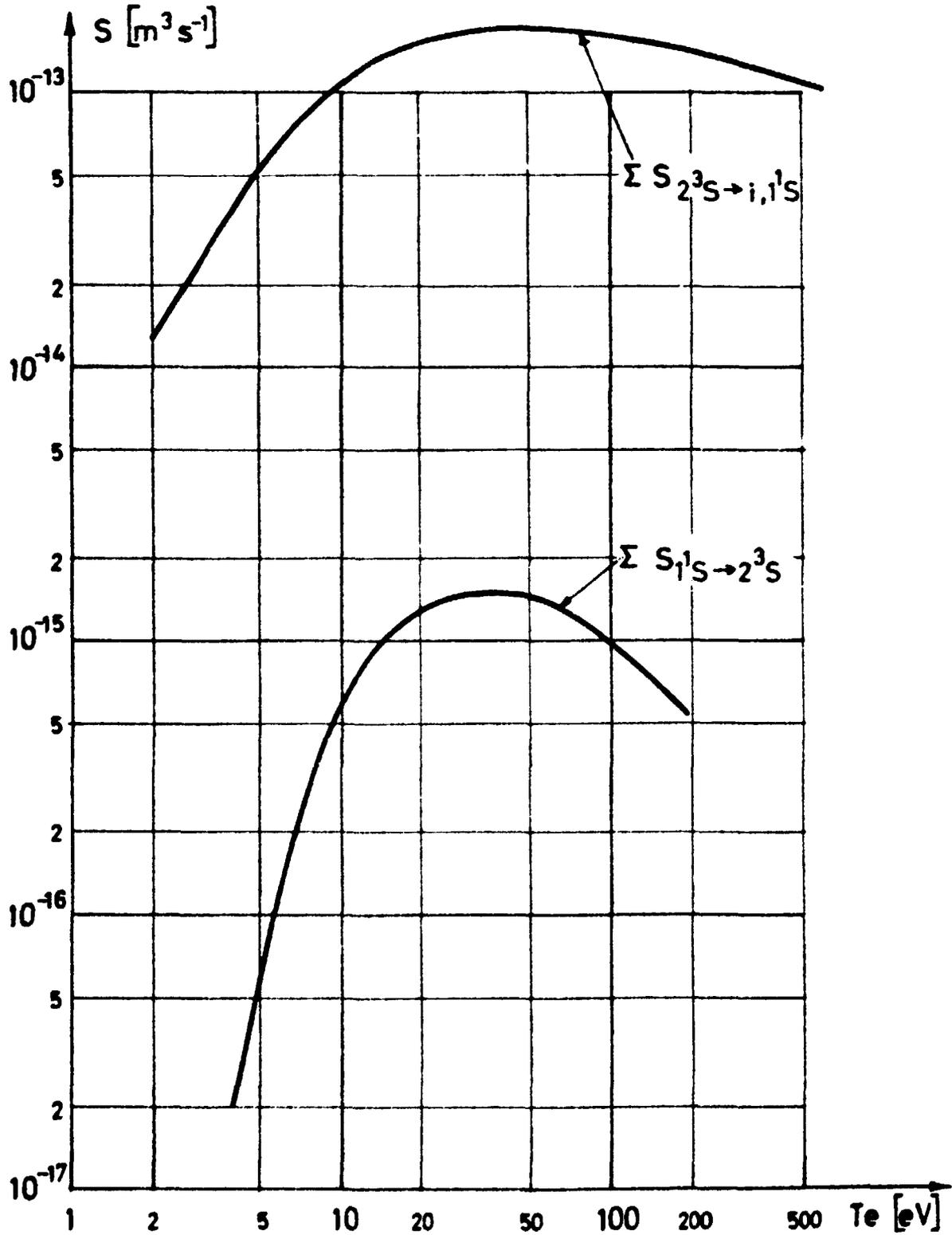
Figure 5. Rate coefficients necessary for the solution of equation (5). $\Sigma \, S_{1^1S \,\rightarrow\, 2^3S}$ denotes the sum of all rate coefficients for all routes of excitation $1^2S \rightarrow 2^3S$, and $\Sigma \, S_{2^3S \,\rightarrow\, i,\, 1^1S}$ denotes the corresponding sum for deexcitation, which gives either an ion or an atom in the 1^1S state.
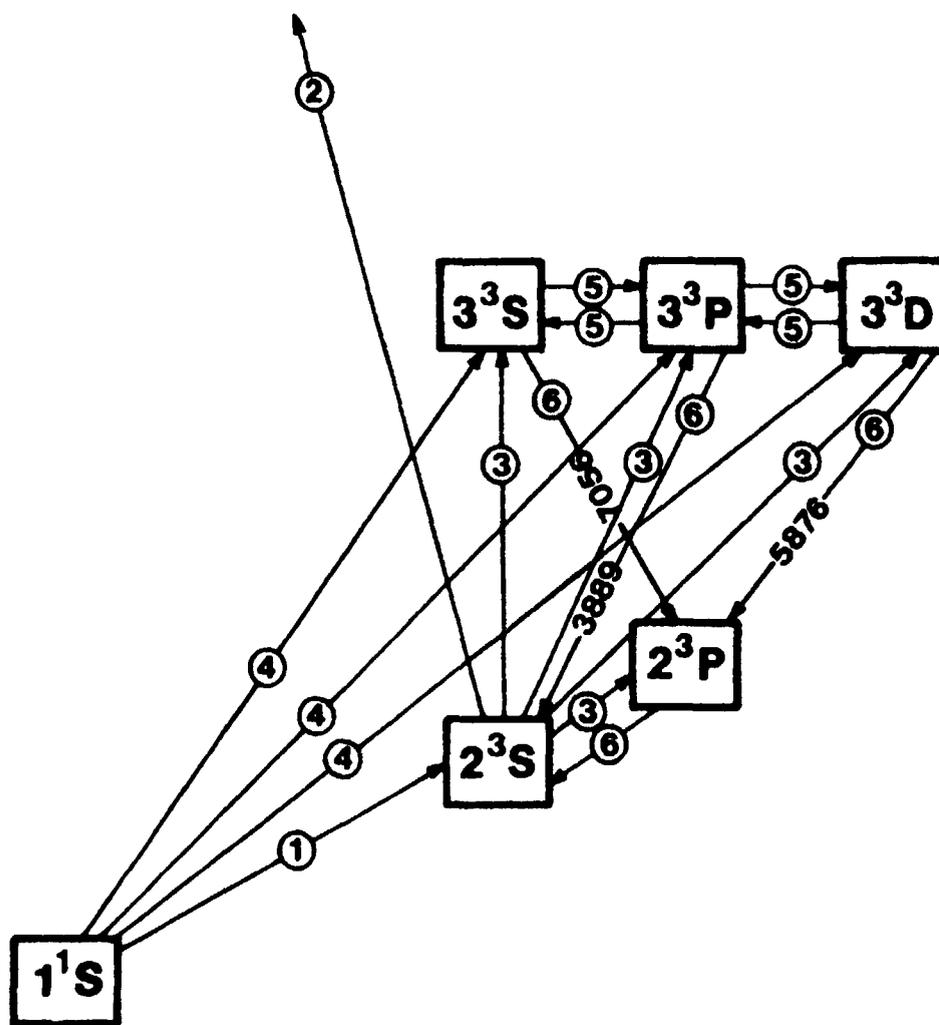
Figure 6a. The processes that determine the 3889Å line excitation rate.

(1) Excitation $1^1S \rightarrow 2^3S$ by electron impact, directly or via other triplet level excitations followed by cascading to 2^3S.

(2) Ionization from 2^3S by electron impact.

(3) Excitation from 2^3S by electron impact.

(4) Excitation from 1^1S by electron impact.

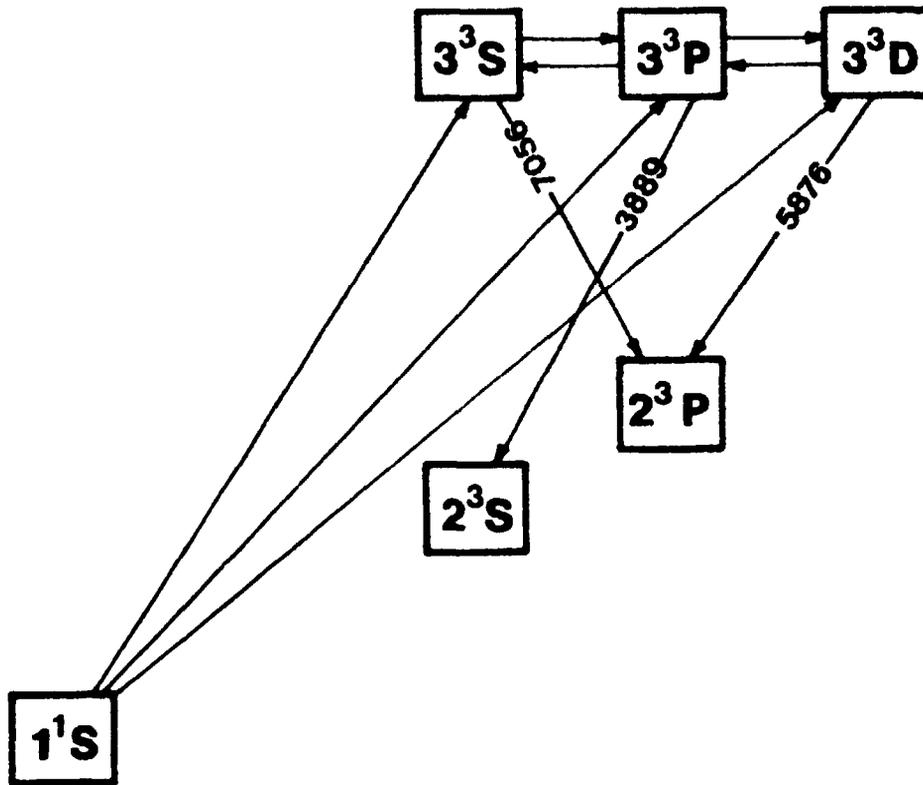(5) Excitation transfer by electron impact.
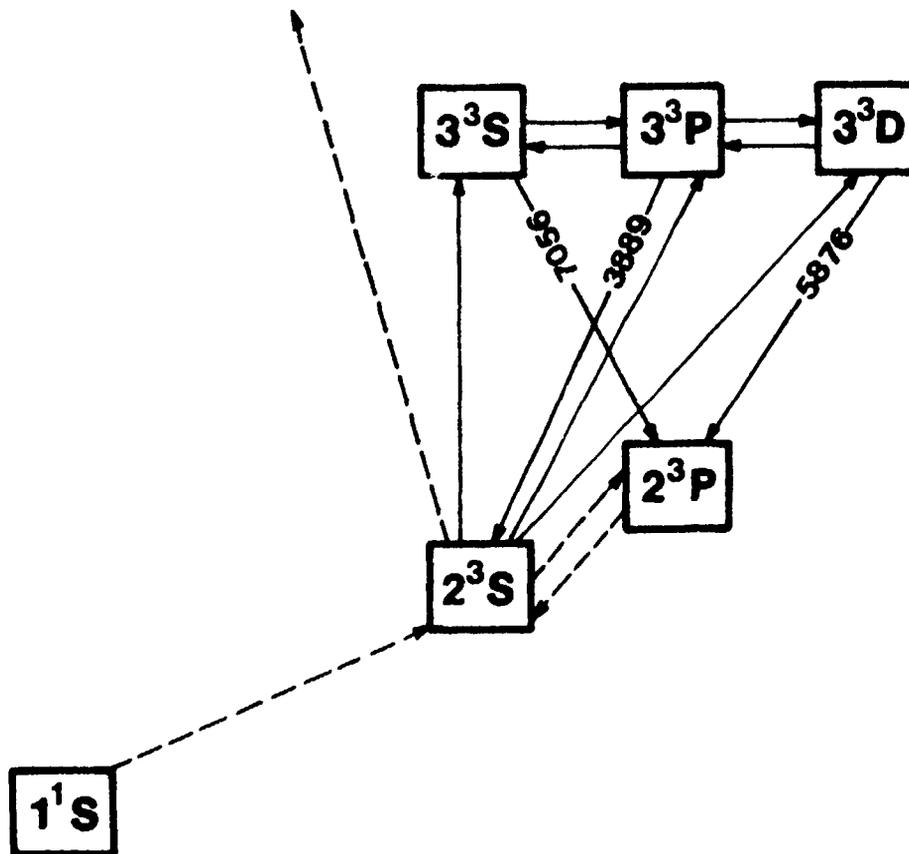
(6) Radiative transitions.

Figure 6b. The processes discussed in Section 2.1.1.
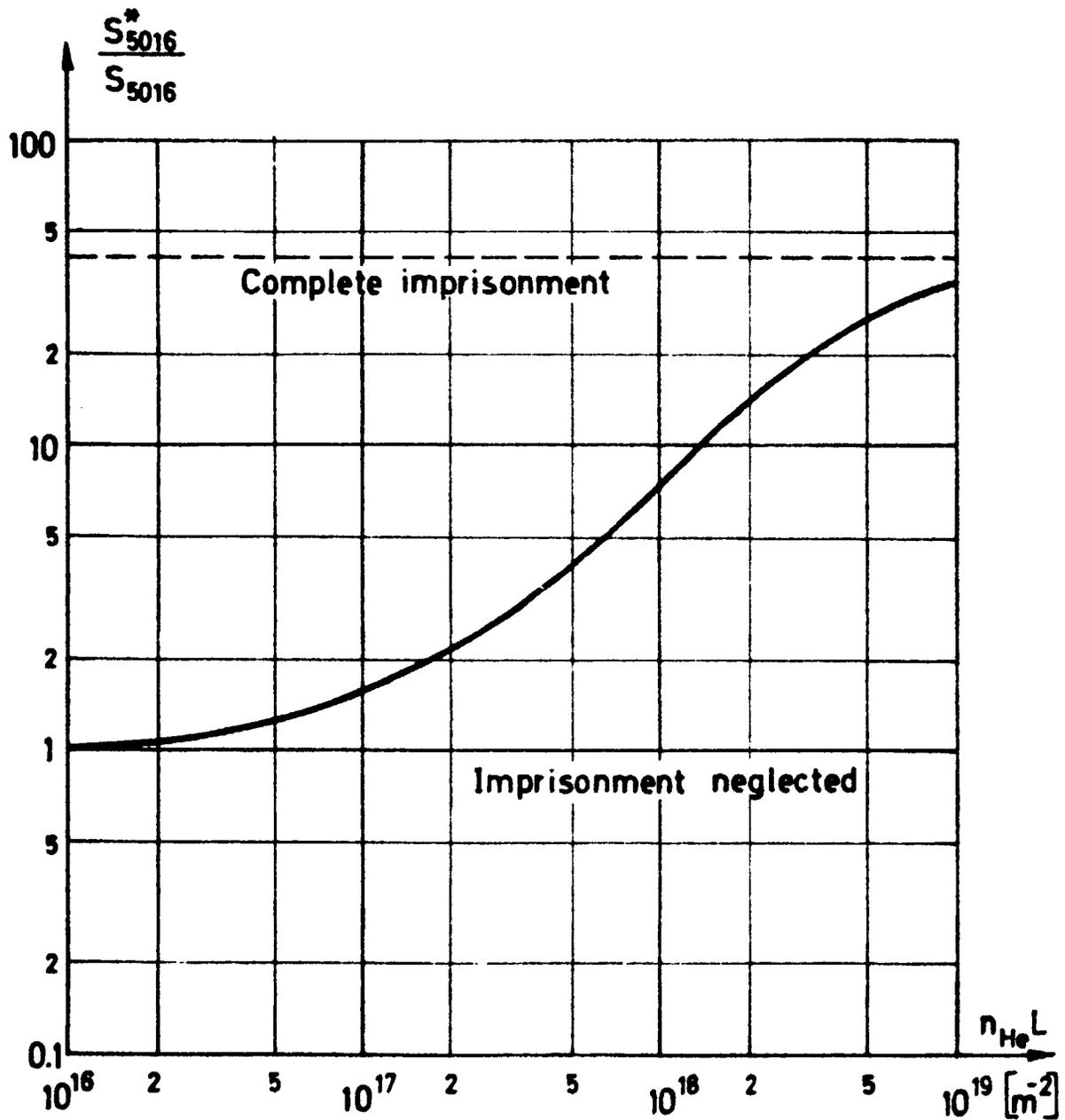

Figure 6c. The processes discussed in Section 2.1.2.

Figure 7. The enhancement of the 5016Å line intensity due to
   imprisonment of resonance radiation. The line emission is ob-
   served perpendicular to a slab of He gas at room temperature witl
   thickness L. The result can be taken as typical for other geo-
   metries, if L is regarded as a characteristic length. From
   Phelps (1958). (Section 3.)
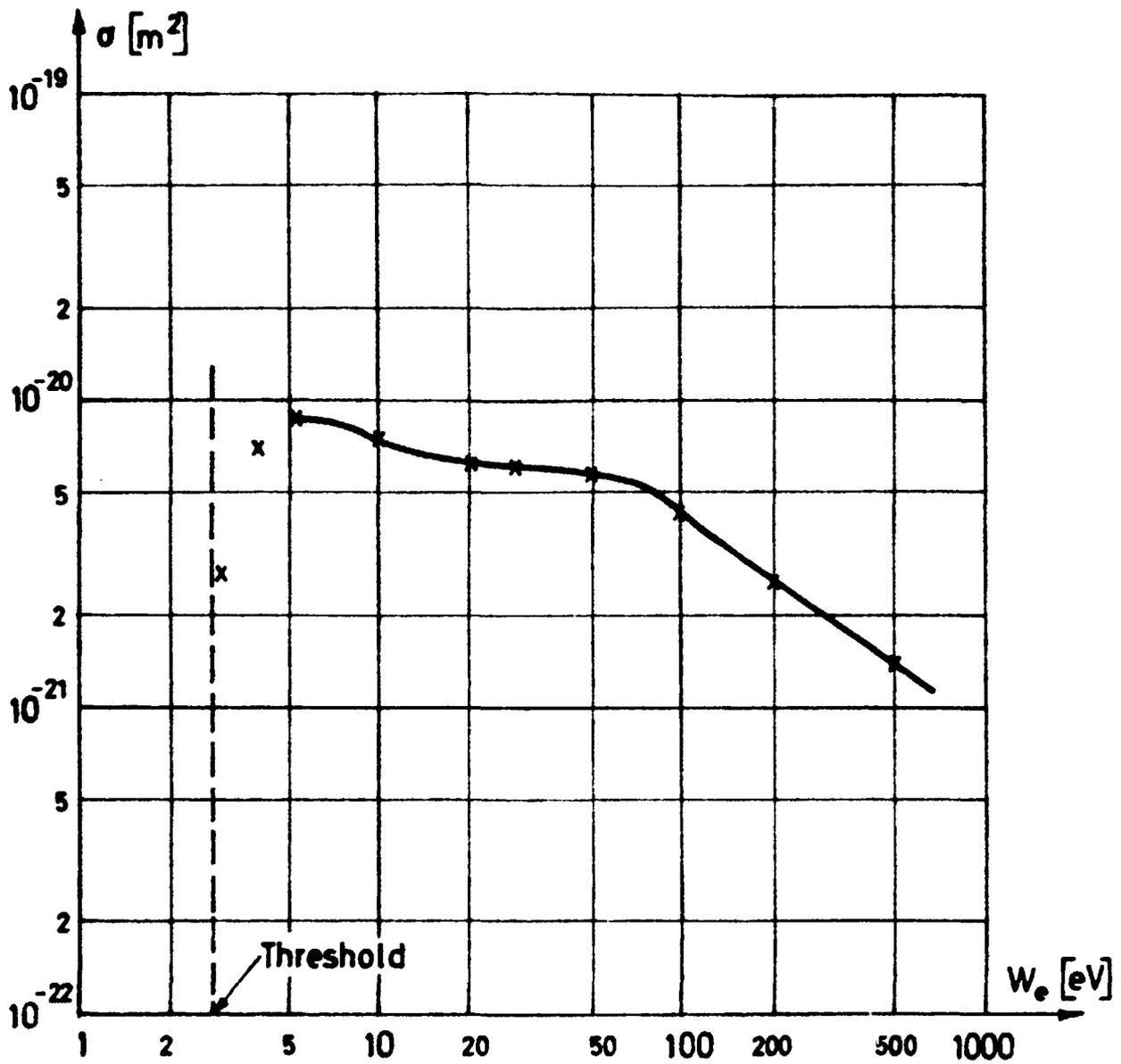
Figure 8. Example of an analytical fit of the type described in Appendix II. This is the cross section for e + He (2^3S) → e + + He (3^3P) excitation. The solid line represents theoretically obtained values (Flannery and Mc Cann, 1975), and the crosses represent the analytical fit.

ELECTRON TEMPERATURE DETERMINATION FROM THE H_e I 3889Å AND
5016Å LINE INTENSITIES

N Brenning

The possibility of determining electron temperature by
helium spectroscopy in low-density ($n_e < 10^{20} m^{-3}$) plasmas is
discussed. It is concluded that most lines can only be used
at very low densities ($n_e < 2 \cdot 10^{16} m^{-3}$) because the line
intensities are highly influenced by secondary processes,
such as electron impact induced transitions between excited
levels or excitations from metastable levels. The density
range where measurements are possible can be extended if the
influence of these secondary processes on the line intensities
can be determined. For most helium I lines this is impossible
for lack of atomic data. However, there are two exceptions,
the 3889Å ($3^1P \rightarrow 2^3S$) and the 5016Å ($3^1P \rightarrow 2^1S$) lines. The
influence from secondary processes on these lines is calculated,
and methods are developed which can be used for measurement
of electron temperatures $T_e < 100$ eV in plasmas of densities
$n_e < 5 \cdot 10^{19} m^{-3}$. The use of the methods is illustrated by a
experiment where they have been successfully applied.

Key words: Helium spectroscopy, Plasma diagnostics, Plasma
            spectroscopy.